



H-Bonded metallomesogens: preparation, characterization, and mesomorphic studies of (3-hydroxypropylimino)propan-1,2-diols

Chieh Chien^c, Chun-Jung Chen^c, Hwo-Shuenn Sheu^a, Gene-Hsiang Lee^b, Chung K. Lai^{c,*}

^a National Synchrotron Radiation Research Center, Hsinchu 30077, Taiwan, ROC

^b Instrumentation Center, National Taiwan University, Taipei 10660, Taiwan, ROC

^c Department of Chemistry, National Central University, Chung-Li 32001, Taiwan, ROC

ARTICLE INFO

Article history:

Received 21 January 2010

Received in revised form 6 March 2010

Accepted 12 March 2010

Available online 20 March 2010

ABSTRACT

Two series of new Schiff bases **2** ($n=8, 12, 16$) derived from (3-hydroxypropyl imino)propan-1, 2-diol with a hydroxyl group at C₁₉/C₂₀-position and their palladium complexes **1** were prepared and their mesomorphic properties investigated by DSC, POM, and XRD. The presence of both hydroxyl groups was found to be crucial in forming the liquid crystalline behavior. All compounds **2a** exhibited smectic A or and C phases, in contrast, all compounds **2b** formed hexagonal columnar phases. The formation of mesophases in both compounds **1–2** was probably induced by inter-molecular H-bonds. Single crystallographic data in mesogenic compound **2a** ($n=8$) indicated that a dimeric structure with a better linear or rod-like molecular shape was formed by an inter-molecular H-bond (O4–O1', ~ 1.854 Å). Another inter-molecular H-bond (~ 1.903 Å) between two dimeric structures was also observed. It crystallizes in a monoclinic space group P2(1)/c. On the other hand, all palladium complexes **1** formed enantiotropic smectic A phases. Single crystallographic data in mesogenic compound **1a** ($n=8$) indicated that the geometry at Pd²⁺ center was coordinated as slightly twisted square planar. It crystallizes in a monoclinic space group P2(1)/n. An inter-molecular H-bond (~ 1.799 Å) between neighboring molecules were observed, which might have facilitated the formation of mesophases. Variable-temperature powder XRD experiments confirmed their mesophase structures.

© 2010 Elsevier Ltd. All rights reserved.

1. Introduction

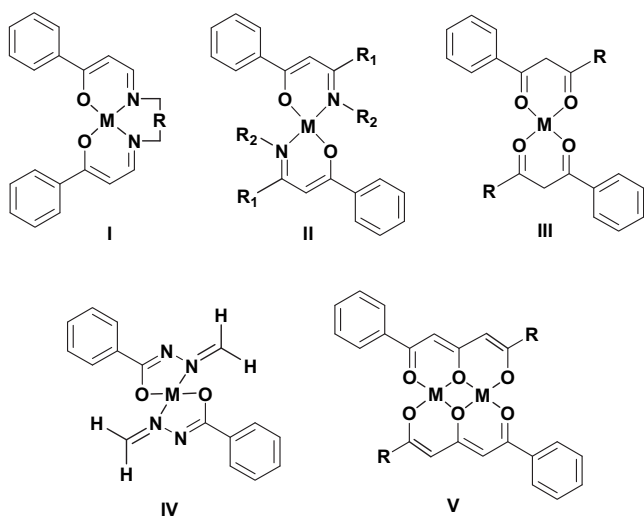
More and more metallomesogens¹ have been prepared and studied during the past decades, and these so-called metal-containing liquid crystals (MCLC's) have now become a major sub-field of long known traditional liquid crystals. More importantly, many interesting LC properties^{1d,2} resulted from such type of metallomesogens were in fact observed, and practical commercial applications on electronic devices might become possible in the near future. We have all been well aware that different mesophases might be formed or induced by distinct molecular shapes/structures. Those specific molecular shapes might not be possible or easy to approach along with classic organic molecules. Metallomesogens were often generated from non-mesogenic moieties. A variety of geometric metal centers within metallomesogenic structures, such as linear, tetrahedron, square planar, octahedron or others have been created. On the other hand, metal ions play an important role in forming the mesophases. Organic moieties or

structures incorporated with atoms capable of binding metal or metals are feasible to generate metallomesogens or poly-metallomesogens. Among them, oxygen, nitrogen, and sulfur atoms were often incorporated due to their nucleophilic or basic properties of lone pair electrons when bonded to more electrophilic or acidic metal ion or ions. Therefore, a delicate balance or control of intermolecular force becomes then crucially important in obtaining the liquid crystalline phases from a particular metal complex. Too strong or too weak a force will destroy its liquid crystallinity.

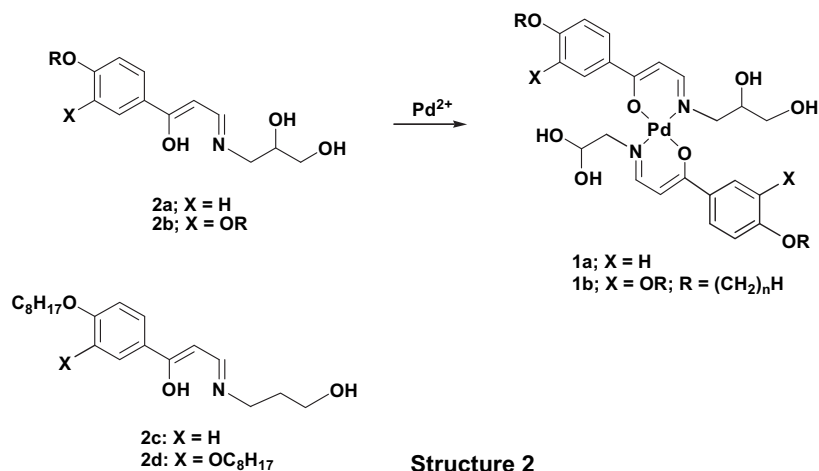
Until now, known metallomesogens derived from enamino-ketonates³ **I**, salicyldimines⁴ **II**, α,β -diketonates⁵ **III**, aroylhydrazines⁶ **IV**, and β,δ -diketonates⁷ **V** were categories investigated the most. Numerous examples of metallomesogens incorporated 3d transition metals exhibiting nematic, smectic or/and columnar phases were by now known. Copper and nickel complexes⁸ similar to compounds **I** with ethylenediamine derivatives ($R=CH_2CH_2$) have been previously studied by this group. All copper complexes regardless of the side chain density were non-mesogenic, however, all nickel complexes with four or six alkoxy groups exhibited columnar phases. The geometry at central metal ion was attributed to the mesomorphic behavior observed by

* Corresponding author. Tel.: +886 03 4259207; fax: +886 03 4277972; e-mail address: ccklai@cc.ncu.edu.tw.

these metal complexes. Diamagnetic nickel ion ($d^8\text{-Ni}^{2+}$) often prefers a square-planar geometry, whereas, paramagnetic copper ion ($d^9\text{-Cu}^{2+}$) tends to be tetrahedral or slightly distorted square plane coordinated.



Structure 1



Structure 2

In this work two new series of *cis*-enaminoketonate derivatives with a hydroxyl group at C₁₉- and C₂₀-position of Schiff bases **2** and their palladium complexes **1** were prepared and mesomorphic properties investigated. The purpose of incorporating hydroxyl groups is to assess its importance or the structural effect on the formation of mesomorphic properties. H-bonds might be possibly formed by these hydroxy groups, and the mesophases could be conceivably induced or formed. Results appeared that all compounds **2a** with one alkoxy group formed smectic A or/and smectic C phases, however, all compounds **2b** with two alkoxy groups exhibited hexagonal columnar (Col_h) phases. On the other hand, all more rod-like palladium complexes **2a,2b** formed smectic A phases. The Pd²⁺ ion with a d^8 -electronic configuration often prefers a diamagnetic state and square-planar geometry. Also in order to understand the relationship between the structure and mesophase, two single crystals **1a** and **2a** all with $n=8$ were resolved and their crystallographic data discussed. A dimeric structure formed by inter-molecular H-bond in compounds **2a**

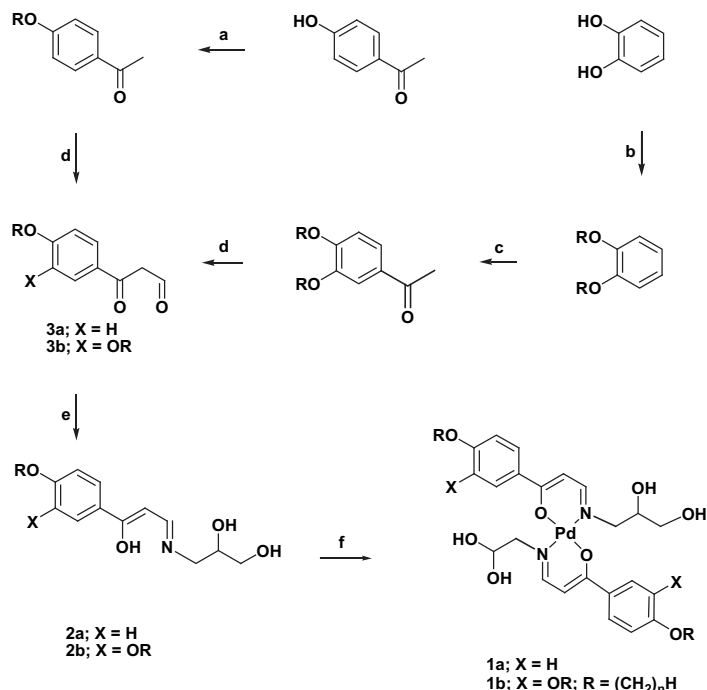
was observed, leading to a better linear shape and improved mesophases induced. An inter-molecular H-bond in compound **1a** ($n=8$) was also observed, by which the formation of the mesophases was facilitated.

H-bonded mesogens⁹ have been an active subfield in liquid crystalline research, and many examples were known. H-bonding has now become an important tool for building molecular architectures with liquid crystalline and/or other optic-electric properties. Induction, stabilization or formation of mesophases by use of H-bonding interaction can be twofold; complementary shapes and intermolecular force. A better molecular shape or an appropriate aspect ratio might be optimized by a H-bonded dimeric, trimeric or polymeric structure, which were often observed for those molecules with unconventionally shaped molecules. Secondly, intermolecular interaction enhanced by H-bond might facilitate the formation of mesophases, particularly for those molecules without a dipole group. H-bonds, compared to covalent bonds are relatively weak; therefore, they are truly sensitive to the structural alternation. Any structural change might have a dramatic impact on the propensity of these H-bond stabilized molecules. On the other hands, known examples of H-bonded metallomesogens^{3b,10} have been relatively described. Studying the relationship between the molecular structure and the mesomorphic properties can therefore provide valuable insight for the design of new LC's materials.

2. Results and discussion

2.1. Synthesis and characterization

The synthetic pathways to compounds **2** and their palladium complexes **1** are listed in Scheme 1. The 4- or 3,4-alkoxyphenyl-3-oxo-3-phenylpropionaldehyde derivatives **3**, obtained by the Claisen formylation reactions were freshly prepared due to their slight sensitivity to the oxidations. These intermediates and Schiff bases were characterized by ¹H and ¹³C NMR spectroscopy. A characteristic peak at ca. δ 9.91–9.93 assigned for aldehyde-H ($-\text{CHO}$) for compounds **3a** and **3b** was observed. In addition, three characteristic peaks at ca. δ 6.70–6.80, 6.83–6.92, and 10.18–10.20 assigned for an olefinic methane-H ($-\text{CH}=\text{C}-$), aldehyde-H ($-\text{CHO}$), and imine-H ($-\text{C}=\text{NH}-$) were observed. The intensities of these peaks were dependent on the solvent and the time length due to the relative tautomeric ratio. Metal complexes, obtained by the reactions of Schiff bases **2** with palladium(II) acetate were



Scheme 1. Reagents and conditions. (a) RBr (1.0 equiv), K₂CO₃ (2.0 equiv), KI, refluxing in acetone, 48 h; (b) RBr (2.0 equiv), K₂CO₃ (3.0 equiv), KI, refluxing in acetone, 48 h; (c) AlCl₃, acetyl chloride, CH₂Cl₂ (dry) at 0 °C, 4 h; (d) NaOMe, DME, HCOOEt, stirring at rt, 24 h; (e) 3-amino-1,2-propanediol (1.1 equiv), refluxing in THF/EtOH, 8 h; (f) Pd(OAc)₂ (0.5 equiv), stirring in THF/MeOH at rt, 3 h.

obtained after twice recrystallizations from THF/methanol. All palladium complexes were isolated as yellow solids. All complexes were all characterized by elemental analysis (Table 5).

2.2. Single crystal structures of 1-(4-octyloxyphenyl)-3-(3-hydroxypropylimino)propan-1,2-diol (2a; *n*=8) and its palladium complex (1a; *n*=8)

In order to understand the relationship between the structure and mesomorphic properties and also the possible effect of the hydroxyl

groups (–OH), two single crystals of the mesogenic ligand **2a** (*n*=8) and its mesogenic palladium complex **1a** (*n*=8) suitable for crystallographic analysis were obtained by slow vaporization from CH₂Cl₂/methanol at room temperature and their structures resolved. As expected, the acidity of primary alcohol–OH at C₂₀ position and secondary alcohol–OH at C₁₉ position of Schiff bases on the Schiff bases are not strong enough to coordinate with softer and larger metal ions, such as Pd²⁺ or Pt²⁺. Instead, imine–N and enaminoketone–O atoms were bonded to Pd²⁺ ion, leaving the two hydroxyl groups uncoordinated. Figure 1 shows the two molecular structures with the

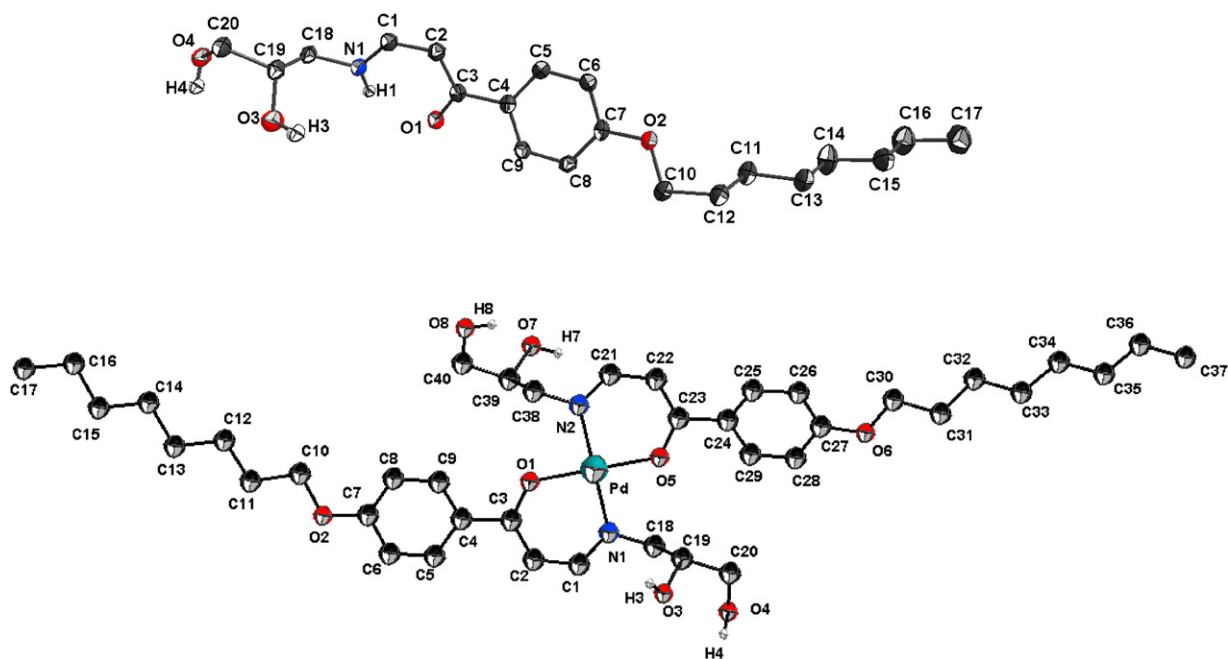


Figure 1. Two ORTEP plots for **2a** (*n*=8; top) and **1a** (*n*=8; bottom) with the numbering scheme, and the thermal ellipsoids of the non-hydrogen atoms are drawn at the 50% probability level.

atomic numbering schemes. Table 1 lists their crystallographic and structural refinement data for the two molecules. The derivative **2a** ($n=8$) crystallizes in a monoclinic space group $P2(1)/c$ with a $Z=4$. The overall molecular shape of crystal **2a** was considered as a slightly bent structure. Unsurprisingly, both inter-molecular H-bond ($H4-O1'$ on C_{20} -position and $H3'-O4$ on C_{19} position) and intra-molecular H-bond ($O1-H1$) were in fact observed. A dimeric structure, leading to a more linear shape was formed by inter-molecular H-bonds, and this was attributed to the formation of a layer smectic phase observed in compounds **2a** (Fig. 2). The two phenyl rings in this dimeric structure were perfectly coplanar. The bond angles of the H-bonds were ranged

Table 1
Crystallographic and experimental data for compounds **1a** and **2a** ($n=8$)

Compd.	2a ($n=8$)	1a ($n=8$)
Empirical formula	$C_{20}H_{31}NO_4$	$C_{41}H_{64}N_2O_9Pd$
Formula weight	349.4	835.34
T/K	150(2)	200(2)
Crystal system	Monoclinic	Monoclinic
Space group	$P2(1)/c$	$P2(1)/n$
$a/\text{\AA}$	20.9194(3)	5.4037(3)
$b/\text{\AA}$	8.6903(2)	18.3223(9)
$c/\text{\AA}$	11.1929(2)	43.315(2)
$\alpha/^\circ$	90	90
$\beta/^\circ$	104.2173(10)	93.4745(16)
$\gamma/^\circ$	90	90
$U/\text{\AA}^3$	1972.50(6)	4280.7(4)
Z	4	4
$F(000)$	760	1768
$D_c/\text{Mg m}^{-3}$	1.177	1.296
Crystal size/ mm^3	$0.33 \times 0.22 \times 0.08$	$0.38 \times 0.06 \times 0.03$
Range for data collection/ $^\circ$	1.00 to 27.50	1.21 to 25.00
Reflection collected	13,566	20,327
Data, restraints, parameters	4533/0/229	7538/1/474
Independent reflection	4533 [$R(\text{int})=0.0365$]	7538 [$R(\text{int})=0.0917$]
Final $R1, wR2$	0.0565, 0.1645	0.0864, 0.2327

between 124.8° ($\angle N1-H1-O1$) and 175.1° ($\angle O4-H4-O1'$). Two hydroxyl groups at C_{19} and C_{20} positions were all responsible for the inter-molecular H-bonds. The distances of two inter-molecular H-bonds were measured as $\sim 1.854 \text{ \AA}$ ($O1'-H4$) and $\sim 1.903 \text{ \AA}$ ($O4-H3'$), whereas the distance of intra-molecular H-bonds was $\sim 2.128 \text{ \AA}$ ($O1-H1$). The inter-molecular H-bonds were relatively stronger than that of the intra-molecular H-bond. In the unit cell, two more linear dimeric structures, shown in Figure 2 were also linked by another H-bond ($O4-H3'$) with a distance of $\sim 1.903 \text{ \AA}$ and bond angle of $\sim 163.7^\circ$ ($\angle O4-H3'-O3'$). This inter-molecular H-bond between two dimeric structures has apparently enhanced the molecular interaction between the layers. The molecular length L of this dimeric structure was measured as ca. $\sim 37.394 \text{ \AA}$, which was slightly less than double lengths of monomeric structure (ca. $\sim 21.724 \text{ \AA}$). The length of 37.394 \AA was quite close to the d-spacing of $\sim 38.239 \text{ \AA}$ obtained by powder XRD diffraction experiment. Therefore, alkoxy chains were probably not interdigitated in the mesophase.

In contrast, the palladium complex **1a** ($n=8$) crystallizes in a monoclinic space group $P2(1)/n$ with a $Z=4$. The geometry at palladium center was coordinated as distorted square planar. The two angles of $N2-Pd-O1$ and $N2-Pd-O5$ were of 87.74° and 92.45° , which were quite close to an angle of 90° expected for a perfect square-planar geometry (see Table 2). The overall molecular shape was considered as slightly bent with a length of ca. 34.957 \AA . Two phenyl rings were not coplanar to the central plane defined by atoms of $N2-O5-Pd-O1-N1$. Two molecules were also linked by H-bonding in a fashion of *anti*-parallel and head-to-tail arrangements. A few inter-molecular H-bonds with a distance ranged between 1.799 and 2.4294 \AA were also observed, which were also attributed to the formation of the mesophase in compounds **1** (Fig. 3). Two types of inter-molecular H-bonds were observed in the unit cell; one formed from neighboring molecule via H atom at C_{19} and O atom at C_{20} , and the other one formed from above or below molecule via H-atom at C_{20} and O-atom at C_{20} . In the unit cell, all molecules were arranged with a herringbone.

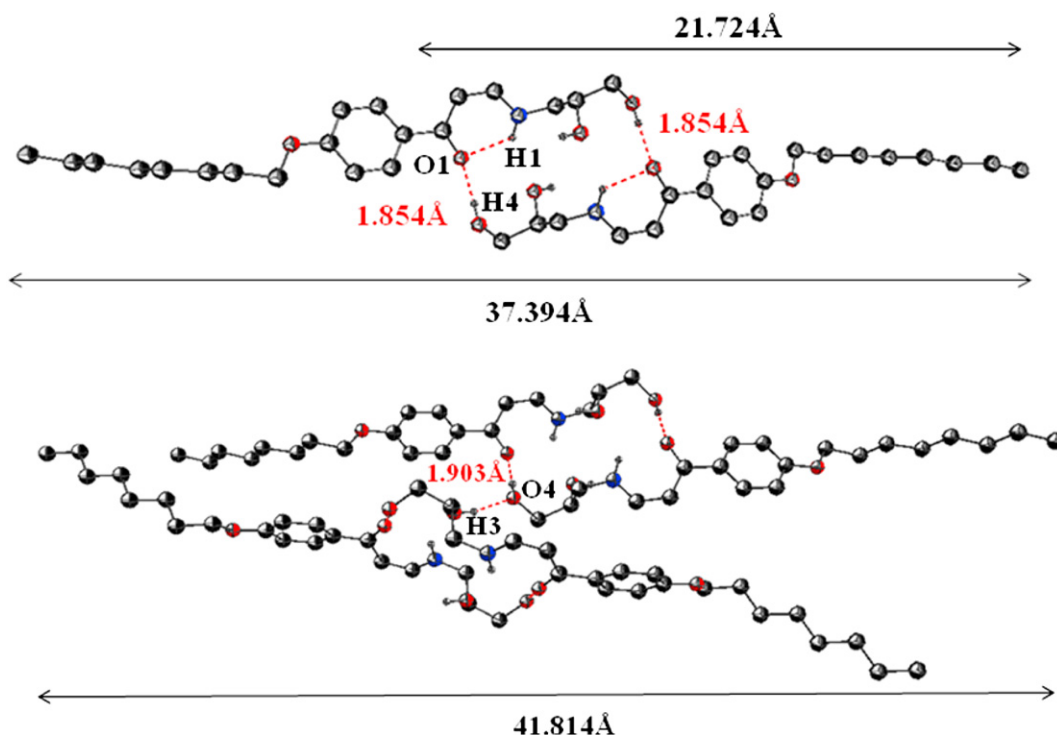


Figure 2. Two H-bonds formed in **2a** ($n=8$). Top plot: inter-molecular ($\sim 1.854 \text{ \AA}$) and intra-molecular ($\sim 2.128 \text{ \AA}$) H-bonds in a dimeric structure, and bottom plot: inter-dimer bond ($\sim 1.903 \text{ \AA}$; H atom on C_{19} and O atom on neighboring C_{20}).

Table 2
Selected bond distances [Å] and angle [°] for compound **2a** and **1a** ($n=8$)

2a			
<i>Bond distances</i>			
C(1)–C(2)	1.3823(24)	C(4)–C(3)	1.4951(24)
C(2)–C(3)	1.4135(26)	N(1)–C(1)	1.3212(22)
C(3)–O(1)	1.2566(21)	N(1)–H(1)	0.8802(16)
<i>Bond angles</i>			
C(1)–C(2)–C(3)	122.568(166)	C(4)–C(3)–O(1)	119.393(156)
C(2)–C(3)–O(1)	121.449(164)	C(1)–N(1)–H(1)	119.402(169)
C(3)–C(4)–C(9)	118.826(157)	C(2)–C(1)–N(1)	128.002(175)
1a			
<i>Bond distances</i>			
N(1)–Pd	2.0087(76)	C(2)–C(3)	1.3767(136)
N(2)–Pd	2.0341(76)	C(3)–O(1)	1.2933(107)
O(1)–Pd	1.9793(65)	C(21)–C(22)	1.3974(142)
O(5)–Pd	2.0010(63)	C(21)–N(2)	1.3163(120)
C(1)–C(2)	1.3871(144)	C(22)–C(23)	1.3682(137)
C(1)–N(1)	1.3164(119)	C(23)–O(5)	1.3173(107)
<i>Bond angles</i>			
N(1)–Pd–O(1)	91.932(276)	C(3)–O(1)–Pd	126.353(551)
N(1)–Pd–O(5)	87.871(273)	C(4)–C(3)–O(1)	113.804(760)
N(2)–Pd–O(1)	87.741(279)	C(21)–N(2)–Pd	121.486(614)
N(2)–Pd–O(5)	92.453(277)	C(21)–N(2)–C(38)	117.014(785)
C(1)–N(1)–Pd	123.093(617)	C(23)–O(5)–Pd	126.185(545)
C(1)–N(1)–C(18)	115.656(786)	C(24)–C(23)–O(5)	113.675(760)

Symmetry transformations used to generate equivalent atoms.

2.3. Mesomorphic properties

The liquid crystalline behavior of compounds **1–2** was characterized and studied by differential scanning calorimetry and polarized optical microscope. The phase transitions and thermodynamic data are summarized in Tables 3 and 4. All three compounds **2a** ($n=8, 12, 16$) with one terminal alkoxy group exhibited enantiotropic

phases, and under optical microscope they exhibited oily streak texture (Fig. 4), characteristic of a layer smectic phase expected for the rod-like molecules. The phases were tentatively assigned as smectic A phases based on POM observation. For the compounds **2a** the clearing temperatures were increased with the carbon numbers of the terminal alkyl chains, i.e. $T_{cl}=154.4$ ($n=8$) < 163.6 ($n=12$) < 167.9 °C ($n=16$), however, the melting temperatures decreased slightly; 124.7 °C ($n=8$)–117.2 °C ($n=16$). The mesophase temperature, also slightly increasing with carbon length was ranged in $\Delta T=29.7$ ($n=8$)–50.7 °C ($n=16$). An extra SmC phase, ranged quite narrow (ca. ~ 2.9 °C) was also observed for compound **2a** with a longer alkoxy ($n=16$). A typical texture described as Schlieren domains (Fig. 4) were easily observed under POM. This may probably be attributed to an enhanced dispersive interaction or van der Waals between the terminal alkoxy chains. The formation of the layer smectic phases was induced by the H-bonding, of which a dimeric structure with a larger aspect ratio facilitated the formation of the mesophases in compound **2a**.

However, all compounds **2b** ($n=8, 12, 16$) with two alkoxy groups formed enantiotropic columnar phases (Col). On DSC thermographs they all showed a typical columnar phase transition, crystal-to-columnar-to-isotropic (Cr \rightarrow Col \rightarrow I). A focal-conic texture for columnar phases (Fig. 4) was observed under POM. The temperature range of columnar phase was narrow and increased with carbon chain length, i.e. $\Delta T=5.70$ °C ($n=8$) < $\Delta T=20.2$ °C ($n=16$) on heating process. In addition, a relatively small enthalpy ($\Delta H=0.43$ –0.88 kJ/mol on heating cycle) for the Col_h \rightarrow I transition was observed, indicating that the molecular order in the columnar phase was relatively low. The overall molecular shapes of compounds **2b** were in fact not disc-like, however, two or more molecules linked or correlated by H-bonds might lead to a more disc-like molecule, giving to the formation of columnar phases. As expected, compounds **2c, 2d** without a hydroxyl group attached at C₁₉-position of Schiff bases

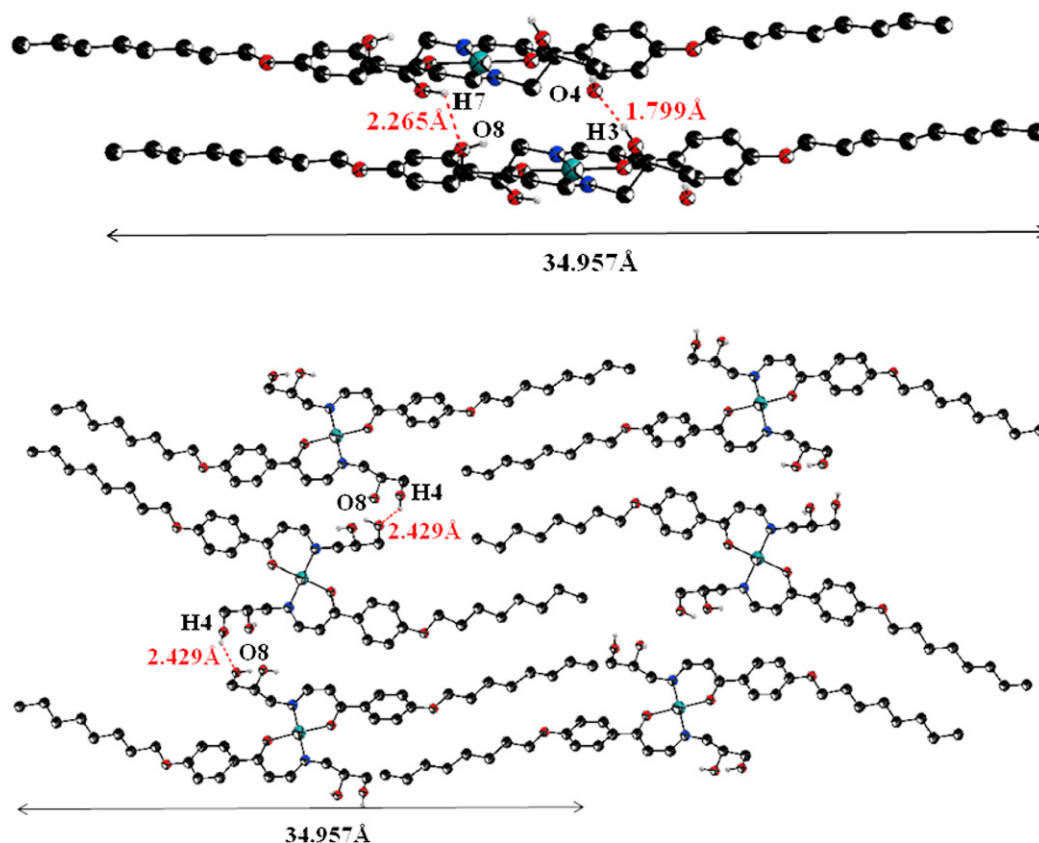


Figure 3. Inter-molecular H-bonds in **1a** ($n=8$) viewed from b axis (top plot) and from a axis (bottom plot).

Table 3
Phase temperatures^a and enthalpies of compound **2a–2d**

2a ; n = 8		Cr ₁	<u>124.7 (58.4)</u>	SmA	<u>154.4 (2.88)</u>	I		
			<u>105.1 (15.7)</u>		<u>151.1 (2.91)</u>			
			<u>123.0 (-5.82)</u>		<u>163.6 (1.68)</u>			
12	Cr ₁		<u>116.7(42.4)</u>	Cr ₂	<u>90.6 (-10.1)</u>	SmA	<u>156.1 (1.46)</u>	I
			<u>86.9 (9.47)</u>			<u>117.2 (57.9)</u>		<u>167.9 (0.96)</u>
16	Cr		<u>101.3 (18.2)</u>	SmC	<u>104.2 (0.18)</u>	SmA	<u>165.1 (0.91)</u>	I
						<u>115.8 (41.4)</u>		<u>121.5 (0.43)</u>
2b ; n = 8		Cr	<u>64.1 (28.7)</u>	Col _h	<u>119.6 (0.55)</u>	I		
			<u>122.5 (-11.1)</u>		<u>141.4 (0.88)</u>			
			<u>90.8 (-13.9)</u>	Col _h	<u>138.6 (0.84)</u>	I		
12	Cr ₁		<u>109.9 (53.2)</u>	Cr ₂	<u>110.3 (70.1)</u>	Col _h	<u>130.5 (0.57)</u>	I
			<u>74.6 (53.1)</u>			<u>124.9 (0.50)</u>		<u>92.6 (25.3)</u>
16	Cr ₁		<u>102.6 (12.3)</u>	Cr ₂	<u>53.5 (5.04)</u>	Cr ₂	<u>78.7 (20.8)</u>	I
			<u>84.4 (82.3)</u>			<u>40.7 (3.62)</u>		<u>89.1 (65.7)</u>
2c		Cr ₁	<u>40.7 (3.62)</u>	Cr ₂	<u>60.5 (53.4)</u>	I		
2d		Cr		Cr		I		

^a n is the carbon numbers of terminal alkoxy groups. Cr₁ and Cr₂=crystal, SmA=smectic A, SmC=smectic C, Col_h=hexahonal columnar, and I=isotropic phase.

Table 4
Phase temperatures^a and enthalpies of compounds **1a–1b**

1a ; n = 8		Cr	<u>186.3 (61.8)</u>	SmA	<u>205.0 (4.72)</u>	I		
			<u>98.6 (32.9)</u>		<u>199.1^b</u>			
			<u>173.8 (65.4)</u>		<u>213.4 (6.00)</u>			
12	Cr		<u>103.8 (29.6)</u>		<u>204.2^b</u>	I		
			<u>164.2 (73.1)</u>		<u>211.5 (6.70)</u>			
16	Cr		<u>120.8 (36.8)</u>	SmA	<u>203.1^b</u>	I		
			<u>148.1 (76.9)</u>		<u>167.3 (6.06)</u>			
1b ; n = 8		Cr	<u>100.2^b</u>	SmA	<u>150.1^b</u>	I		
			<u>130.9 (5.0)</u>		<u>148.4 (4.41)</u>			
			<u>115.4 (64.2)</u>		<u>137.6 (3.29)</u>			
12	Cr ₁		<u>125.0 (56.50)</u>	Cr ₂	<u>115.4 (64.2)</u>	SmA	<u>126.5 (1.90)</u>	I
			<u>56.1^b</u>			<u>73.6 (37.2)</u>		<u>118.9 (2.29)</u>
16	Cr ₁		<u>86.2 (-19.6)</u>	Cr ₂	<u>115.4 (64.2)</u>	SmA	<u>126.5 (1.90)</u>	I
			<u>73.6 (37.2)</u>			<u>118.9 (2.29)</u>		

^a n is the carbon numbers of terminal alkoxy groups. Cr₁, Cr₂=crystal, SmA=smectic A, and I=isotropic phase.

^bobserved by optical microscope.

Table 5
Elemental analysis data of compounds **1–2**

Compds	C (%)	H (%)
2a (n=8)	68.39 (68.74)	8.92 (8.94)
2a (n=12)	71.04 (71.07)	9.75 (9.69)
2a (n=16)	72.90 (72.84)	10.35 (10.26)
2b (n=8)	70.31 (70.40)	9.88 (9.92)
2b (n=12)	73.32 (73.30)	10.79 (10.76)
2b (n=16)	75.29 (75.27)	11.40 (11.34)
1a (n=8)	59.80 (59.79)	7.58 (7.53)
1a (n=12)	63.01 (62.97)	8.34 (8.33)
1a (n=16)	65.37 (65.44)	9.02 (9.02)
1b (n=8)	62.99 (63.47)	8.74 (8.75)
1b (n=12)	67.12 (67.34)	9.69 (9.73)
1b (n=16)	69.77 (70.06)	10.44 (10.42)

Theoretical values in parenthesis.

were found to be non-mesogenic. A transition from crystal-to-isotropic at 92.6 °C and 89.1 °C for compound **2c** and **2d**, respectively was obtained. A decreasing of clearing temperatures for compound **2c** and **2d** by a ΔT_{cl} =61.8 °C and 32.4 °C, respectively, with respect to those of **2a** (n=8) and **2b** (n=8). The loss of LC behavior might be attributed to the weakening of the H-bond interaction induced only at C₂₀-position. The phase transitions and thermodynamic data of compounds **1** are summarized in Table 4. All

compounds **1a** have a higher clearing temperature than those of compounds **2a** (n=8) by ca. 43.6 °C–50.6 °C. In contrast, for the compounds **1b** only the derivative (n=8) has a higher clearing isotropic temperature than that of its precursor **2b** (n=8) by 45.8 °C. The other two derivatives **1b** (n=12, 16) have slightly lower clearing temperatures than that those of their precursors **2b** (n=12, 16). All palladium complexes **1a,1b** formed layer smectic phases. The phases were identified also as smectic A phases, and typical focal-conic textures (Fig. 5) were easily observed under optical polarized microscope when cooling from isotropic liquid. All compounds **1a** have a smaller range of mesophase temperature.

2.4. Variable-temperature powder XRD diffraction data

The mesophase structures for some of the compounds **1a,1b** and **2a,2b** were also confirmed by use of variable-temperature powder XRD experiments. For example, for compound **2a** (n=8) at 125.0 °C a diffraction pattern with one strong peak of d ~ 38.2 Å and one very weak of d ~ 19.1 Å at small angle region, and also a very weak and broad halo diffraction peak of d ~ 4.4 Å at wide angle region was observed, as shown in Figure 6. These two diffraction peaks at lower angle were assigned as 001 and 002, which were typically characteristics of layer structures observed for a SmA phase. The layer d-spacing

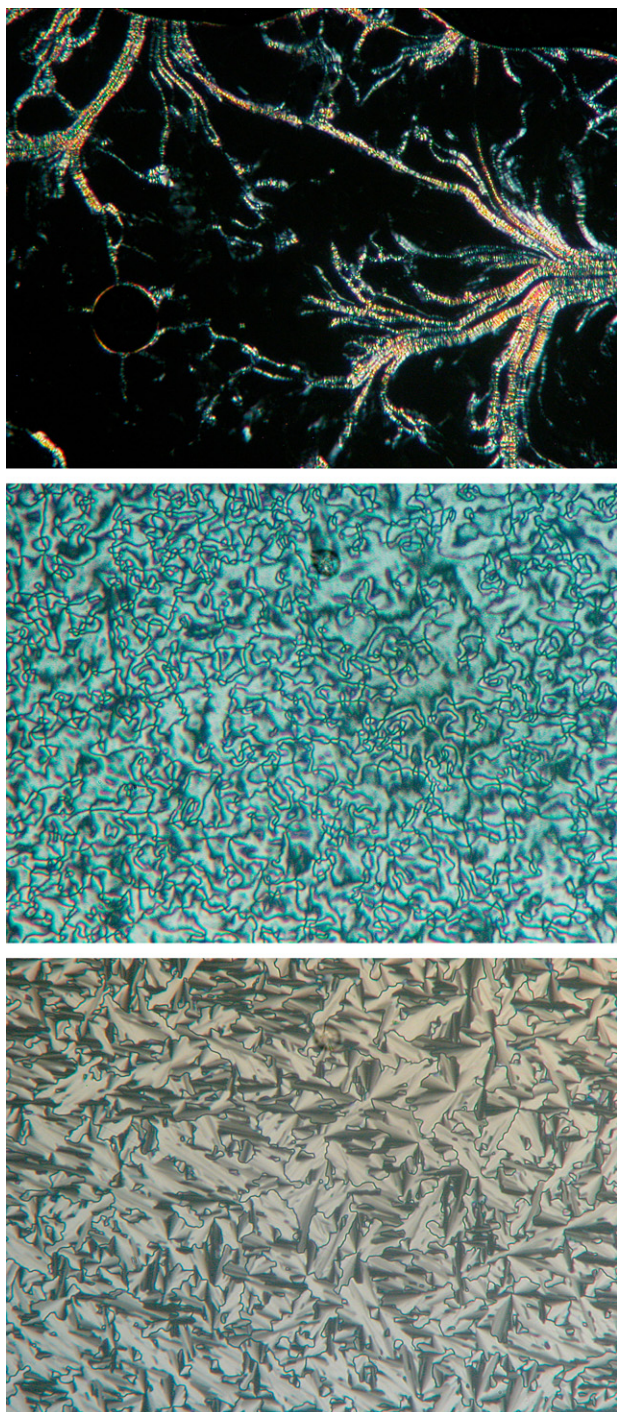


Figure 4. Optical textures observed by **2a** ($n=16$) at 157.0 °C (top) and at 103.0 °C (center), and by **2b** ($n=16$) at 122.8 °C (bottom).

of 38.2 Å is quite consistent to a distance of ~ 37.4 Å obtained for the molecular length of the dimeric structure in single crystallographic data of **2a** ($n=8$), which indicates that the formation of a smectic phase was induced or/and formed by a H-bonded dimeric structure. In addition, all alkoxy chains were not probably interdigitated.

In contrast, all compounds **2b** ($n=8, 12, 15$) exhibited columnar phases based on polarized optical microscope. At 110 °C, a diffraction pattern of compound **2b** ($n=8$) with a d-spacing at 34.5 Å, 19.9 Å, 17.2 Å, and a broad diffuse peak at 4.4 Å at wide-angle region was observed, and it is characteristic of a columnar phase with a d-spacing ratio of 1, $(1/3)^{1/2}$ and $(1/4)^{1/2}$, corresponding to Miller indices, 10, 11, and 20, respectively. Such diffraction pattern

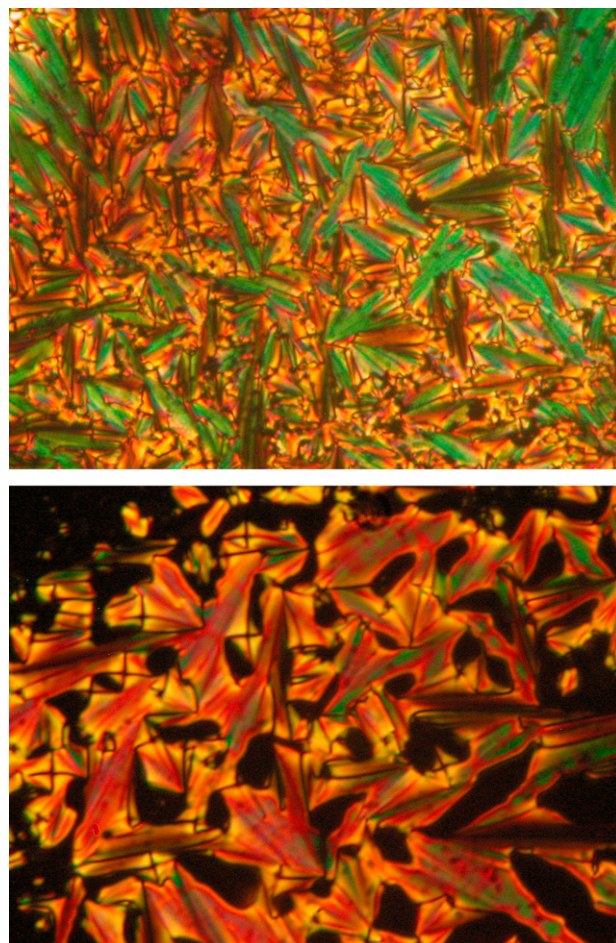


Figure 5. Optical textures observed by **1a** ($n=12$) at 191.0 °C (top) and by **1b** ($n=8$) at 112.0 °C.

corresponds to a hexagonal columnar (Col_h) arrangement¹¹ with a lattice constant ($a=2 \cdot d_{10}/3^{1/2}$) of ~ 39.8 Å. This lattice constant was also quite close to the 35.0 Å obtained for the molecular length in single crystallographic data of **1b** ($n=8$). The overall molecular shapes of compounds **2b** were not considered as disc-like, but a more lath-like. However, a correlated structure having two or more molecules with a 180° or antiparallel arrangement would lead to a more disc-like molecule, giving a columnar phase.

The powder XRD data measured for compounds **1a** ($n=8$) at 180 °C and **1b** ($n=8$) at 155.0 °C confirmed the layer structures of smectic A phases, the same with compound **2a**. For example, a diffraction pattern with a peak at 32.1 Å (assigned as d_{001}), 16.0 Å (d_{002}) and also a halo peak at 4.4 Å was observed as shown in Figure 7. Compound **1b** ($n=8$) showed a similar diffraction pattern with a peak at 29.7 Å (d_{001}), 15.0 Å (d_{002}), 10.0 Å (d_{003}) and 4.4 Å (halo). The molecular arrangements of compounds **2a** and **1a** both in crystal and smectic A phases are proposed in Figure 8.

3. Conclusions

Two series of new Schiff bases **2** and their palladium complexes **1** were prepared and their mesomorphic properties investigated. The presence of two hydroxyl groups attached at Schiff base C₁₉- and C₂₀-position is crucial in forming the liquid crystalline behavior. Two single crystallographic data of compounds **2a** and **1a** ($n=8$) confirmed their single and molecular structures. A dimeric structure induced by inter-molecular H-bond was attributed to the formation of mesophases in compounds **2**. All compounds **2a**

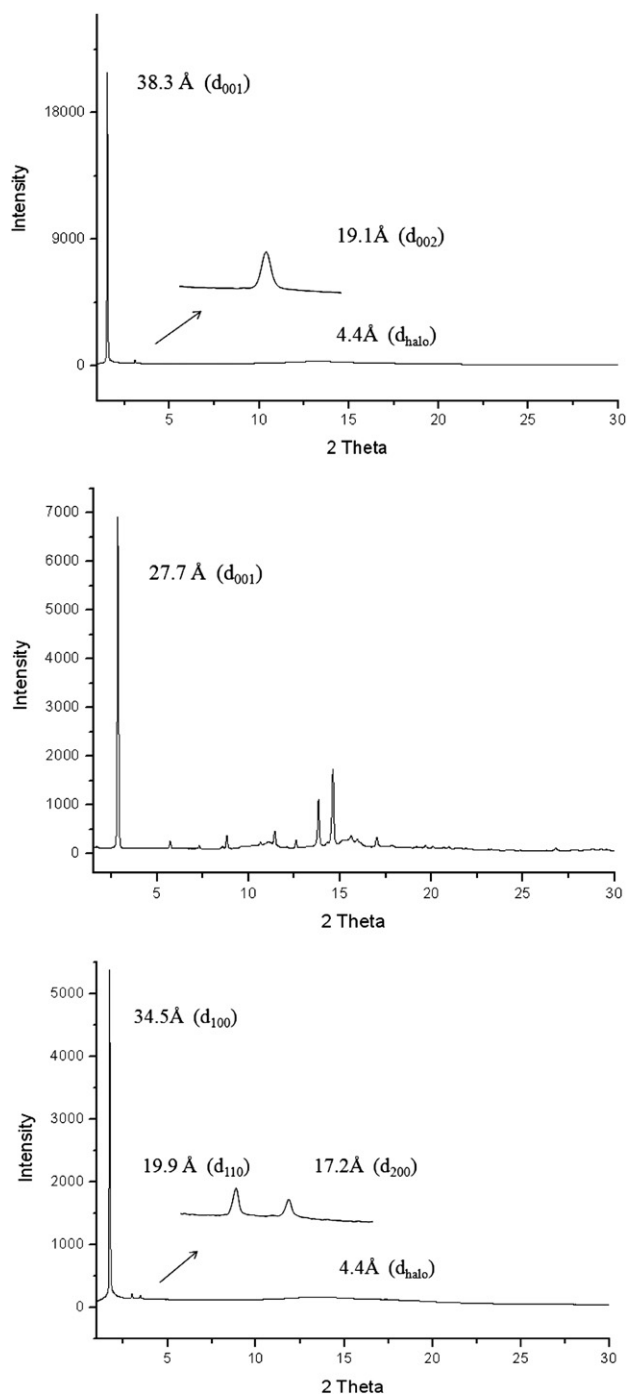


Figure 6. The powder X-ray diffraction plots of compound **2a** ($n=8$) at 125.0 °C (top) and at rt, and compound **2b** ($n=8$) at 110.0 °C (bottom).

exhibited smectic A or/and C phases, in contrast, all compounds **2b** formed hexagonal columnar phases.

4. Experiment section

4.1. General

The ^1H and ^{13}C NMR spectra were measured on a Bruker DRS-200. DSC thermographs were carried out on a Mettler DSC 1 Star System. All phase transitions are determined by a scan rate of 10.0 °C/min. Optical polarized microscope was carried out on Zeiss Axioplan 2 equipped with a hot stage system of Mettler FP90/FP82HT. Elemental analysis for carbon, hydrogen, and nitrogen were

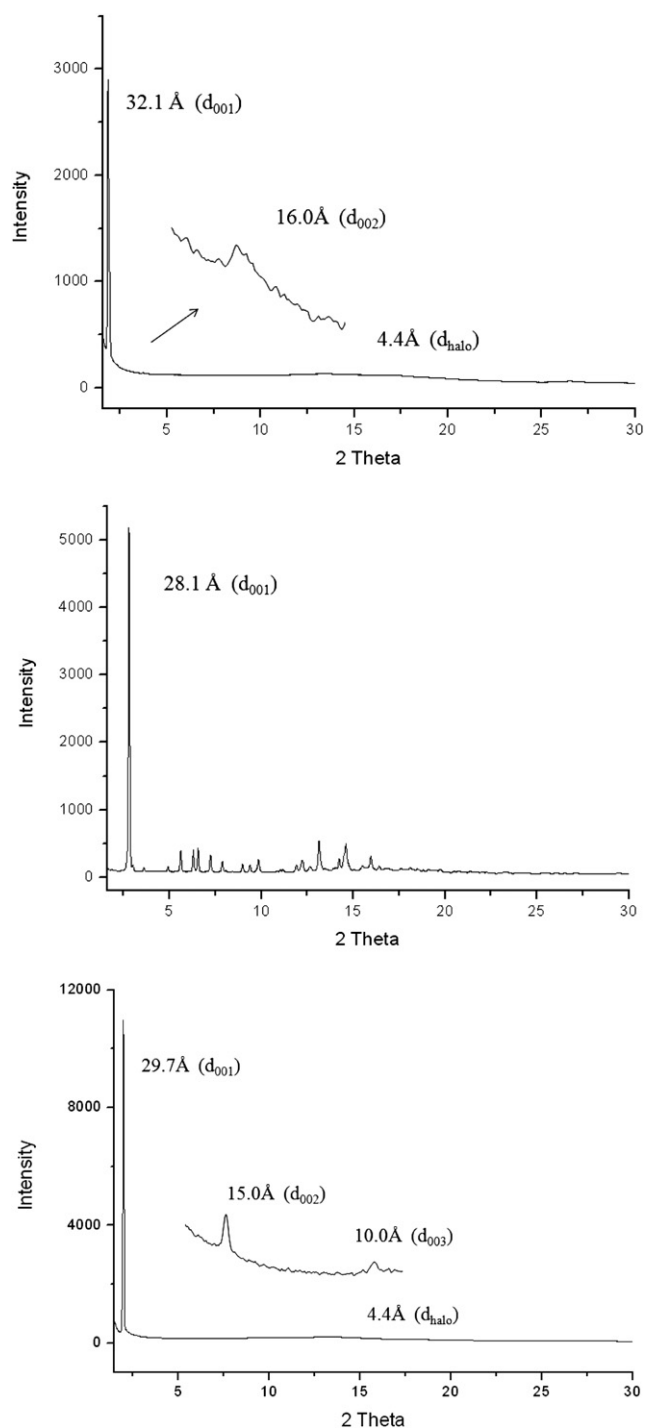


Figure 7. The powder X-ray diffraction plots of compound **1a** ($n=8$) at 180.0 °C (top) and at rt, and compound **1b** ($n=8$) at 155.0 °C (bottom).

conducted at Instrumentation Center, National Taiwan University on a Heraeus CHN-O-Rapid elemental analyzer. The powder X-ray diffraction data were collected from the Wiggler-A beam line of the National Synchrotron Radiation Research Center. All compounds of 4-alkoxyacetophenones and 3,4-dialkoxyacetophenones were prepared by literatures' procedures.

4.1.1. 1-(4-Octyloxyphenyl)-3-hydroxy-2-propen-1-one (3a; $n=8$). Light yellow solid, ^1H NMR (300 MHz, CDCl_3): δ 0.85 (t, 3H, $-\text{CH}_3$, $J=6$ Hz), 1.24–1.81 (m, 12H, $-\text{CH}_2$), 3.98 (t, 2H, $-\text{OCH}_2$, $J=7$ Hz), 6.12 (d, 1H, CH, $J=4$ Hz), 6.90 (d, 2H, $-\text{C}_6\text{H}_4$, $J=7$ Hz), 7.84 (d, 2H,

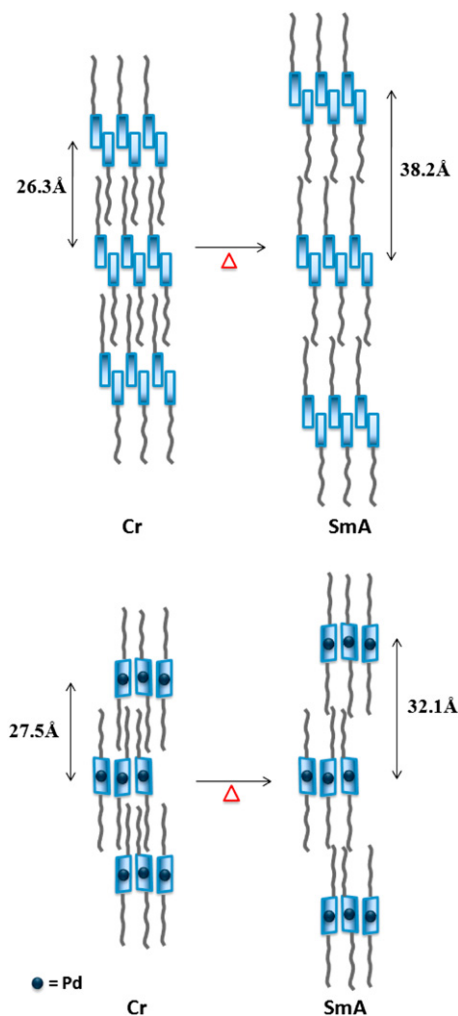


Figure 8. Molecular arrangements proposed for compound **2a** ($n=8$, top) and **1a** ($n=8$, bottom) both in crystal phase and smectic A phases. The two d-spacings used in Cr phases were obtained from XRD data measured at rt (see Figs. 6 and 7).

–C₆H₄, $J=7$ Hz), 8.10 (d, 1H, –(CO)CH, $J=4$ Hz), 9.92 (s, –COH, 1H). ¹³C NMR (75 MHz, CDCl₃): δ 14.04, 22.60, 25.93, 29.04, 29.16, 29.26, 31.75, 68.18, 68.27, 68.35, 97.65, 114.34, 114.43, 129.56, 163.18, 176.50, 188.11.

4.1.2. *1-(4-Dodecyloxyphenyl)-3-hydroxy-2-propen-1-one (3a; n=12)*. Light yellow solid, ¹H NMR (300 MHz, CDCl₃): δ 0.86 (t, 3H, –CH₃, $J=7$ Hz), 1.24–1.82 (m, 20H, –CH₂), 3.99 (t, 2H, –OCH₂, $J=6$ Hz), 6.12 (d, 1H, CH, $J=4$ Hz), 6.91 (d, 2H, –C₆H₄, $J=9$ Hz), 7.85 (d, 2H, –C₆H₄, $J=9$ Hz), 8.10 (d, 1H, –(CO)CH, $J=4$ Hz), 9.93 (s, –COH, 1H). ¹³C NMR (75 MHz, CDCl₃): δ 14.05, 22.63, 25.91, 29.03, 29.29, 29.50, 29.52, 29.58, 31.86, 68.25, 97.62, 114.41, 127.37, 129.53, 130.76, 163.16, 176.46, 188.09.

4.1.3. *1-(4-Hexadecyloxyphenyl)-3-hydroxy-2-propen-1-one (3a; n=16)*. Light yellow solid, ¹H NMR (300 MHz, CDCl₃): δ 0.86 (t, 3H, –CH₃, $J=7$ Hz), 1.24–1.83 (m, 28H, –CH₂), 3.99 (t, 2H, –OCH₂, $J=7$ Hz), 6.13 (d, 1H, CH, $J=4$ Hz), 6.91 (d, 2H, –C₆H₄, $J=9$ Hz), 7.85 (d, 2H, –C₆H₄, $J=9$ Hz), 8.11 (d, 1H, –(CO)CH, $J=4$ Hz), 9.93 (s, –COH, 1H). ¹³C NMR (75 MHz, CDCl₃): δ 14.09, 22.67, 25.95, 29.07, 29.34, 29.54, 29.56, 29.67, 31.91, 68.30, 97.67, 114.45, 127.42, 129.58, 130.81, 162.92, 163.20, 176.51, 188.14.

4.1.4. *1-(3,4-Bis(octyloxy)phenyl)-3-hydroxyprop-2-en-1-one (3b; n=8)*. White solid, ¹H NMR (300 MHz, CDCl₃): δ 0.86 (t, –CH₃,

6H, $J=6$ Hz), 1.27–1.87 (m, –CH₂, 24H), 4.03 (t, –OCH₂, 4H, $J=4$ Hz), 6.13 (d, –(COH)CH, 1H, $J=4$ Hz), 6.86 (d, –C₆H₃, 1H, $J=4$ Hz), 7.45–7.47 (m, –C₆H₃, 2H), 8.03 (d, –(CO)CH, 1H, $J=4$ Hz), 9.92 (s, –COH, 1H). ¹³C NMR (75 MHz, CDCl₃): δ 14.07, 22.66, 25.97, 26.00, 29.06, 29.19, 29.26, 29.34, 31.81, 69.08, 69.36, 97.85, 112.05, 112.16, 121.85, 127.84, 149.03, 153.62, 175.49, 188.81.

4.1.5. *1-(3,4-Bis(dodecyloxy)phenyl)-3-hydroxyprop-2-en-1-one (3b; n=12)*. White solid, ¹H NMR (300 MHz, CDCl₃): δ 0.86 (t, –CH₃, 6H, $J=6$ Hz), 1.24–1.84 (m, –CH₂, 40H), 4.03 (t, –OCH₂, 4H, $J=4$ Hz), 6.13 (d, –(COH)CH, 1H, $J=4$ Hz), 6.86 (d, –C₆H₃, 1H, $J=4$ Hz), 7.45–7.49 (m, –C₆H₃, 2H), 8.03 (d, –(CO)CH, 1H, $J=4$ Hz), 9.92 (s, –COH, 1H). ¹³C NMR (75 MHz, CDCl₃): δ 14.01, 22.60, 25.89, 25.92, 28.97, 29.11, 29.28, 29.54, 31.84, 69.00, 69.27, 97.76, 111.96, 112.07, 121.76, 127.76, 148.94, 153.53, 175.40, 188.74.

4.1.6. *1-(3,4-Bis(hexadecyloxy)phenyl)-3-hydroxyprop-2-en-1-one (3b; n=16)*. White solid, ¹H NMR (300 MHz, CDCl₃): δ 0.86 (t, 6H, –CH₃, $J=6$ Hz), 1.24–1.845 (m, 56H, –CH₂), 1.79–1.84 (m, 2H, –CH₂), 4.03 (t, 2H, –OCH₂, $J=6$ Hz), 6.13 (d, 1H, –(COH)CH, $J=4$ Hz), 6.85 (d, 1H, Ar–H, $J=8$ Hz), 7.44–7.48 (m, 2H, Ar–H), 8.03 (d, 1H, –(COH)CH, $J=4$ Hz), 9.91 (s, 1H, –COH). ¹³C NMR (75 MHz, CDCl₃): δ 14.10, 22.69, 25.99, 26.01, 29.07, 29.20, 29.38, 29.72, 31.94, 69.07, 69.35, 97.83, 112.04, 112.16, 121.84, 127.83, 149.03, 153.62, 175.51, 188.77.

4.1.7. *1-(4-Hexadecyloxyphenyl)-3-(3-hydroxypropylimino)propan-1,2-diol (2a; n=16)*. The solution of 4'-hexadecyloxy-2-hydroxyacrylophenone (1.0 g, 2.57 mmol) dissolved in 15 mL of dry THF was slowly added 3-amino-1,2-propanediol (0.223 g, 2.45 mmol) dissolved in 10 mL of abs 10 ethanol under nitrogen atmosphere. The mixture was stirred at room temperature for 8 h. The solution was concentrated to dryness. The product, isolated as white solid was obtained after recrystallization from CH₃OH/THF. Yield 64–70%. ¹H NMR (300 MHz, CDCl₃): δ 0.86 (t, 3H, –CH₃, $J=7$ Hz), 1.18–1.77 (m, 28H, –CH₂), 2.17 (s, 1H, –OH), 2.81 (s, 1H, –OH), 3.28–3.38 (m, 2H, –NCH₂), 3.49–3.84 (m, 3H, –CH(OH)CH₂(OH)), 3.97 (t, 2H, –OCH₂, $J=4$ Hz), 5.68 (d, 1H, CH, $J=4$ Hz), 6.87 (d, 2H, –C₆H₄, $J=4$ Hz), 6.92 (m, 1H, –CHN), 7.81 (d, 2H, –C₆H₄, $J=4$ Hz), 10.20 (m, 1H, –COH).

4.1.8. *1-(4-Octyloxyphenyl)-3-(3-hydroxypropylimino)propan-1,2-diol (2a; n=8)*. Off-white solid, ¹H NMR (300 MHz, CDCl₃): δ 0.85 (t, 3H, –CH₃, $J=4$ Hz), 1.26–1.76 (m, 12H, –CH₂), 2.43 (s, 1H, –OH), 3.05 (s, 1H, –OH), 3.28–3.35 (m, 2H, –NCH₂), 3.61–3.83 (m, 3H, –CH(OH)CH₂(OH)), 3.95 (t, 2H, –OCH₂, $J=4$ Hz), 5.67 (d, 1H, CH, $J=4$ Hz), 6.66 (d, 2H, –C₆H₄, $J=4$ Hz), 6.90 (d, 1H, –CHN), 7.80 (d, 2H, –C₆H₄, $J=4$ Hz), 10.20 (m, 1H, –COH). ¹³C NMR (75 MHz, CDCl₃): δ 14.07, 15.26, 22.64, 25.53, 26.01, 27.20, 29.20, 29.32, 29.47, 31.79, 51.57, 63.97, 68.13, 71.43, 90.57, 114.02, 121.49, 128.61, 129.02, 132.00, 154.33, 161.75, 189.66, 192.85, 216.76.

4.1.9. *1-(4-Dodecyloxyphenyl)-3-(3-hydroxypropylimino)propan-1,2-diol (2a; n=12)*. Off-white solid, ¹H NMR (300 MHz, CDCl₃): δ 0.86 (t, 3H, –CH₃, $J=4$ Hz), 1.24–1.77 (m, 20H, –CH₂), 2.50 (s, 1H, –OH), 3.25 (s, 1H, –OH), 3.25–3.41 (m, 2H, –NCH₂), 3.56–3.83 (m, 3H, –CH(OH)CH₂(OH)), 3.96 (t, 2H, –OCH₂, $J=4$ Hz), 5.67 (d, 1H, CH, $J=4$ Hz), 6.87 (d, 2H, –C₆H₄, $J=4$ Hz), 6.91 (d, 1H, –CHN), 7.80 (d, 2H, –C₆H₄, $J=4$ Hz), 10.18 (m, 1H, –COH). ¹³C NMR (75 MHz, CDCl₃): δ 14.09, 15.26, 22.68, 26.00, 29.19, 29.33, 29.58, 29.63, 31.91, 51.55, 63.96, 68.12, 71.43, 90.58, 114.01, 129.01, 132.00, 147.26, 154.29, 161.74, 189.65.

4.1.10. *1-(3,4-Octyloxyphenyl)-3-(3-hydroxypropylimino)propan-1,2-diol (2b; n=8)*. Light yellow solid, ¹H NMR (300 MHz, CDCl₃): δ 0.86 (t, 6H, –CH₃, $J=3$ Hz), 1.23–1.75 (m, 24H, –CH₂), 1.98 (s, 1H,

–OH), 2.71 (s, 1H, –OH), 3.29–3.33 (m, 2H, –NCH₂), 3.57–3.83 (m, 3H, –CH(OH)CH₂(OH)), 4.00 (t, 2H, –OCH₂, *J*=3 Hz), 5.67 (d, 1H, CH, *J*=4 Hz), 6.82 (d, 1H, –C₆H₄, *J*=4 Hz), 6.84–6.91 (d, 1H, –CHN), 7.39–7.44 (m, 2H, –C₆H₄), 10.18 (m, 1H, –COH). ¹³C NMR (75 MHz, CDCl₃): δ 14.09, 22.67, 25.95, 29.07, 29.34, 29.54, 29.56, 29.67, 31.91, 68.30, 97.67, 114.45, 127.42, 129.58, 130.81, 162.92, 163.20, 176.51, 188.14.

4.1.11. 1-(3,4-Dodecyloxy phenyl)-3-(3-hydroxypropylimino)propan-1,2-diol (**2b**; *n*=12). Light yellow solid, ¹H NMR (300 MHz, CDCl₃): δ 0.86 (t, 6H, –CH₃, *J*=4 Hz), 1.23–1.75 (m, 40H, –CH₂), 2.54 (s, 1H, –OH), 3.16 (s, 1H, –OH), 3.27–3.37 (m, 2H, –NCH₂), 3.60–3.83 (m, 3H, –CH(OH)CH₂(OH)), 4.01 (t, 4H, –OCH₂, *J*=3 Hz), 5.67 (d, 1H, CH, *J*=4 Hz), 6.82 (d, 1H, –C₆H₄, *J*=4 Hz), 6.88 (d, 1H, –CHN) 7.39–7.45 (m, 2H, –C₆H₄), 10.18 (m, 1H, –COH). ¹³C NMR (75 MHz, CDCl₃): δ 14.10, 22.68, 26.04, 28.18, 29.17, 29.36, 29.42, 29.64, 31.92, 51.60, 64.00, 69.08, 69.27, 71.44, 90.59, 112.17, 112.38, 120.80, 148.76, 154.34.

4.1.12. 1-(3,4-Hexadecyloxyphenyl)-3-(3-hydroxypropylimino)propan-1,2-diol (**2b**; *n*=16). Light yellow solid, ¹H NMR (300 MHz, CDCl₃): δ 0.84 (t, 6H, –CH₃, *J*=4 Hz), 1.14–1.60 (m, 56H, –CH₂), 2.13 (s, 1H, –OH), 2.86 (s, 1H, –OH), 3.26–3.34 (m, 2H, –NCH₂), 3.35–3.47 (m, 3H, –CH(OH)CH₂(OH)), 4.01 (t, 4H, –OCH₂, *J*=3 Hz), 5.68 (d, 1H, CH, *J*=4 Hz), 6.71 (d, 1H, –C₆H₄, *J*=4 Hz), 6.83–6.92 (d, 1H, –CHN) 7.39–7.46 (m, 2H, –C₆H₄), 10.18 (m, 1H, –COH). ¹³C NMR (75 MHz, CDCl₃): δ 14.10, 22.68, 26.00, 29.36, 29.70, 31.92, 66.38, 69.07, 90.58, 112.15, 112.37, 120.81, 189.63.

4.1.13. Palladium complex of 1-(4-octyloxyphenyl)-3-(3-hydroxypropylimino)propan-1,2-diol (**1a**; *n*=8). The solution of 1-(4-octyloxyphenyl)-3-(3-hydroxypropylimino)propan-1,2-diol (0.50 g, 1.43 mmol) dissolved in 10 mL of dry THF and palladium (II) acetate Pd(OAc)₂ (0.168 g, 0.75 mmol) in 10 mL was mixed and then gently refluxed for 3 h. The solution was concentrated to dryness, and the product isolated as yellow solids was obtained after recrystallization from CH₃OH/THF. Yield 82–85%.

Acknowledgements

We thank the National Science Council of Taiwan, ROC (NSC98-2815-C-008-021-M & NSC98-2752-M-008-010-PAE) in generous support of this work.

References and notes

- (a) *Metallomesogens. Synthesis, Properties and Applications*; Serrano, J. L., Ed.; VCH: Weinheim, Germany, 1996; (b) Bruce, D. W. In *Inorganic Materials*, 2nd ed.; Bruce, D. W., O'Hare, D., Eds.; Wiley: Chichester, UK, 1996; Chapter 8, p 429; (c) Donnio, B.; Bruce, D. W. *Struct. Bond.* **1999**, *95*, 193–247; (d) Binnemans, K.; Görlner-Walrand, C. *Chem. Rev.* **2002**, *102*, 2303–2346; (e) Donnio, B.; Guillon, D.; Deschenaux, R.; Bruce, D. W. In *Comprehensive Coordination Chemistry II*; McCleverty, J. A., Meyer, T. J., Eds.; Elsevier: Oxford, 2003; Vol. 7, Chapter 7.9, pp 357–627.
- (a) Binnemans, K. *J. Mater. Chem.* **2009**, *19*, 448–453; (b) Galyametdinov, Y. G.; Knyazev, A. A.; Dzhabbarov, V. I.; Cardinaels, T.; Driesen, K.; Görlner-Walrand, C.; Binnemans, K. *Adv. Mater.* **2008**, *20*, 252–257; (c) Cavero, E.; Uriel, S.; Romero, P.; Serrano, J. L.; Gimenez, R. *J. Am. Chem. Soc.* **2007**, *129*, 11608–11618; (d) Escande, A.; Guenee, L.; Nozary, H.; Bernardinelli, G.; Gumy, F.; Aebischer, A.; Bünzli, J. C. G.; Donnio, B.; Guillon, D.; Piguet, C. *Chem.—Eur. J.* **2007**, *13*, 8696–8713; (e) Piguet, C.; Bünzli, J.-C. G.; Donnio, B.; Guillon, D. *Chem. Commun.* **2006**, 3755–3768; (f) Terazzi, E.; Suarez, S.; Torelli, S.; Nozary, H.; Imbert, D.; Mamula, O.; Rivera, J. P.; Guillet, E.; Benech, J. M.; Bernardinelli, G.; Scopelliti, R.; Donnio, B.; Guillon, D.; Bünzli, J.-C. G.; Piguet, C. *Adv. Funct. Mater.* **2006**, *16*, 157–168.
- (a) Glębowska, A.; Przybylski, P.; Winek, M.; Krzyczkowska, P.; Krwczynski, A.; Szydłowska, J.; Pocięcha, D.; Górecka, E. *J. Mater. Chem.* **2009**, *19*, 1395–1398; (b) Pietrasik, U.; Szydłowska, J.; Krwczynski, A. *Chem. Mater.* **2004**, *16*, 1485–1492; (c) Yang, C. D.; Pang, Y. S.; Lai, C. K. *Liq. Cryst.* **2001**, *28*, 191–195; (d) Lai, C. K.; Lin, R.; Lu, M. Y.; Kao, K. C. *J. Chem. Soc., Dalton Trans.* **1998**, 1857–1862.
- (a) Rzvani, Z.; Divband, B.; Abbasi, A. R.; Nejati, K. *Polyhedron* **2006**, *25*, 1915–1920; (b) Abe, Y.; Nakabayashi, K.; Matsukawa, N.; Takashima, H.; Iida, M.; Tanase, T.; Sugibayashi, M.; Mukai, B.; Ohta, K. *Inorg. Chim. Acta* **2006**, *359*, 3934–3946; (c) Nejati, K.; Rzvani, Z. *New J. Chem.* **2003**, *27*, 1665–1669; (d) Ku, S. M.; Wu, C. Y.; Lai, C. K. *J. Chem. Soc., Dalton Trans.* **2000**, 3491–3492; (e) Hoshino, N. *Coord. Chem. Rev.* **1998**, *174*, 77–108; (f) Lai, C. K.; Chang, C. H.; Tsai, C. K. *J. Mater. Chem.* **1998**, *8*, 599–602.
- (a) Chien, C. W.; Liu, K. T.; Lai, C. K. *J. Mater. Chem.* **2003**, *13*, 1588–1595; (b) Lai, C. K.; Pan, H. B.; Yang, L. F.; Liu, K. T. *Liq. Cryst.* **2001**, *28*, 97–101; (c) Trzaska, S. T.; Zheng, H.; Swager, T. M. *Chem. Mater.* **1999**, *11*, 130–134; (d) Trzaska, S. T.; Hsu, H. F.; Swager, T. S. *J. Am. Chem. Soc.* **1999**, *121*, 4518–4519; (e) Trzaska, S. T.; Swager, T. M. *Chem. Mater.* **1998**, *10*, 428–443; (f) Zheng, H.; Xu, B.; Swager, T. M. *Chem. Mater.* **1996**, *8*, 907–911.
- Lai, C. K.; Tsai, C. H.; Pang, Y. S. *J. Mater. Chem.* **1998**, *8*, 1355–1360.
- (a) Lin, R.; Tsai, C. H.; Chao, M. Q.; Lai, C. K. *J. Mater. Chem.* **2001**, *11*, 359–363; (b) Lai, C. K.; Chen, F. G.; Ku, Y. J.; Tsai, C. H.; Lin, R. *J. Chem. Soc., Dalton Trans.* **1997**, 4683–4687.
- Lai, C. H.; Pang, Y. S.; Tsai, C. H. *J. Mater. Chem.* **1998**, *8*, 2605–2610.
- (a) Coco, S.; Cordovilla, C.; Domínguez, C.; Donnio, B.; Espinet, P.; Guillon, D. *Chem. Mater.* **2009**, *21*, 3282–3289; (b) Lavigueur, C.; Foster, E. J.; Williams, V. E. *J. Am. Chem. Soc.* **2008**, *130*, 11791–11800; (c) Barberá, J.; Puig, L.; Romero, P.; Serrano, J. L.; Sierra, T. *J. Am. Chem. Soc.* **2006**, *128*, 4487–4492.
- (a) Vera, F.; Serrano, J. L.; Sierra, T. *Chem. Soc. Rev.* **2009**, *38*, 781–796; (b) Wang, Y. U.; Song, J. H.; Lin, Y. S.; Lin, C.; Sheu, H. S.; Lee, G. H.; Lai, C. K. *Chem. Commun.* **2006**, 4912–4914; (c) Massiot, P.; Impéror-Clerc, M.; Veber, M.; Deschenaux, M. *Chem. Mater.* **2005**, *17*, 1946–1951; (d) Ziessel, R.; Pickaert, G.; Camerel, F.; Donnio, B.; Guillon, D.; Cesario, M.; Prange, T. *J. Am. Chem. Soc.* **2004**, *126*, 12403–12413.
- (a) Laschat, S.; Baro, A.; Steinke, N.; Giesselmann, F.; Hägele, C.; Scalia, G.; Judele, R.; Kapatsina, E.; Sauer, S.; Schreivogel, A.; Tosonim, M. *Angew. Chem., Int. Ed.* **2007**, *46*, 4832–4887; (b) Kumar, S. *Chem. Soc. Rev.* **2006**, *35*, 83–109.